Journal of Applied Electrochemistry **34**: 841–848, 2004.

Preparation and characterisation of electrodeposited Ni–Cu/Cu Multilayers

M. ALPER[1,*], M.C. BAYKUL[2], L. PÉTER[3] J. TÓTH[3] and I. BAKONYİ[3]
[1]*Department of Physics, Faculty of Sciences and Arts, Uludag University.16059, Görükle, Bursa, Turkey*
[2]*Department of Physics, Faculty of Sciences and Arts, Osmangazi University.26480, Meşelik, Eskişehir, Turkey*
[3]*Research Institute for Solid State Physics and Optics, Hungarian Academy of Sciences. H-1525 Budapest, P.O.B. 49, Hungary*
*(*author for correspondence, e-mail: malper@uludag.edu.tr)*

Received 25 November 2003; accepted in revised form 12 March 2004

Key words: electrodeposition, electrolyte pH, GMR, Ni–Cu/Cu multilayers, superparamagnetism

Abstract

Ni–Cu/Cu multilayers have been, grown from a single electrolyte under potentiostatic conditions at different electrolyte pH values. The current-time transients recorded during deposition indicated different growth modes of the Ni–Cu layers. Structural characterisation by X-ray diffraction revealed that the multilayers have the same crystal structure and texture as their (1 0 0) textured polycrystalline Cu substrate. Scanning electron microscopy showed that the films grown at low pH (2.2) have smoother surfaces than those grown at high pH (3.0). Energy dispersive X-ray analysis revealed that the magnetic layers of the multilayers electrodeposited at high pH contain much more Cu compared to those deposited at low pH. Anisotropic magnetoresistance was found for nominal Cu layer thicknesses below 0.6 nm, and giant magnetoresistance (GMR) above 0.6 nm. The shape of the magnetoresistance curves for GMR multilayers indicated the predominance of a superparamagnetic contribution, possibly due to the discontinuous nature of the magnetic layer. For multilayers with the same bilayer and total thicknesses, the GMR magnitude decreased as the electrolyte pH increased. Besides possible structural differences, this may have come from a strong increase in the Cu content of the magnetic layers since this causes a nearly complete loss of ferromagnetism at room temperature.

1. Introduction

Over the last 10 years, magnetic multilayers which exhibit the giant magnetoresistance (GMR) effect, have been the subject of numerous studies because they have great potential for technological applications such as magnetoresistive sensors and magnetic recording devices. Although such nanostructured materials are generally produced by high-vacuum techniques such as sputtering and molecular beam epitaxy, electrodeposition has also been an alternative technique. The electrodeposition of multilayers has been reviewed [1, 2].

Electrodeposited multilayers can have a structural quality comparable to those of the multilayers grown by vacuum techniques. X-ray diffraction (XRD) showed that some electrodeposited multilayers can exhibit satellite peaks up to the fifth order [3] in the high-angle region and Bragg peaks up to the sixth order [4] in the low-angle region. In spite of this, the GMR magnitudes measured for electrodeposited multilayers [2, 5–8] have remained below the value observed in sputtered multilayers of the same composition [9].

The properties of the multilayer deposits are significantly affected by parameters such as the electrolyte concentration, the electrolyte pH, the deposition potentials, additives, substrates and the control methods (galvanostatic and potentiostatic). The effect of these parameters has been studied extensively [6, 10–19]. In particular, electrolyte pH was found to have a strong effect on the GMR magnitude of electrodeposited Co–Ni–Cu/Cu [15] and Co–Cu/Cu [18] multilayers. Multilayers grown from electrolytes with low pH (below 2) have larger GMR magnitudes than those from electrolytes with high pH (3.0).

As to the Ni–Cu/Cu system, several papers described the observation of GMR in these electrodeposited multilayers [7, 11, 20–25]. In this study, Ni–Cu/Cu multilayers were grown on polycrystalline Cu substrates from a single electrolyte having different pH values in a system similar to those described in previous work [2, 3, 15]. Here, we describe the results of chemical analysis as well as structural and magnetotransport characteristics and discuss the observed variation of GMR with electrolyte pH.

2. Experimental procedures

Polycrystalline Cu sheets having a strong (1 0 0) texture were used as substrate. One face of each substrate specimen was polished mechanically using silicon carbide papers of successively increasing grades, and then masked with electroplating tape except for a circular area ($\sim$3 cm^2) of the polished face. The uncovered area was electropolished in 50 wt.% H_3PO_4 solution. As soon as the polishing process was completed, the substrate was immediately placed into the electrolyte. The electrolyte was similar to that used by Lashmore et al. [26] and contained 2.0 mol dm^{-3} nickel sulfamate [from crystalline $Ni(SO_3NH_2)_2 \times 4H_2O$], 0.04 mol dm^{-3} copper sulfate [from $CuSO_4 \times 5H_2O$] and 0.5 mol dm^{-3} boric acid [H_3BO_3] prepared with distilled water. The deposition was carried out in a 3-electrode cell using a potentiostat (EGG Model 362). A Pt sheet was used as counter electrode (anode). The cathode (working electrode or substrate) potentials are referenced to a saturated calomel electrode (SCE). During deposition, the process was controlled by a personal computer (PC) with in house software. The computer integrates the net current passed between the anode and the cathode. When this current reaches the charge value corresponding to the desired thickness of the particular layer being deposited, the computer changes the cathode potential to deposit the other component. Deposition of Cu layers was carried out at a cathode potential of -0.2 V (vs SCE), while for deposition of magnetic Ni–Cu layers the potential was -1.7 V vs. SCE.

The electrolyte pH was lowered in steps from its initial value of 3.35–2.00 by passing current through the bath as described previously [15]. The electrolysis was carried out by using a sufficiently high current in order to ensure that the metal deposited during pH adjustment was almost exclusively Ni. Hence, neither the Cu^{2+} content of the bath nor the ion concentration ratio changed due to pH adjustment. A series of multilayer samples was prepared. The electrolyte temperature was held at 30 $\pm$ 1 °C. The number of bilayers was chosen to give a total thickness of about 1 μm for each multilayer, except for the XRD samples which were grown up to 2 μm.

The structure of the multilayers was studied on their substrates using a Rigaku Rint-2200 X-ray diffractomer with Cu K_α radiation (λ=1.5406 Å). The diffraction patterns were obtained in the range of 2θ=40°–60° with a step of $\Delta(2\theta)$=0.02°. The surface morphology of the solution side of the multilayers was examined with a Philips XL 30S scanning electron microscope (SEM).

The deposits still on their Cu substrates were then mounted onto a glass sheet using a tape resistant to acidic etch. The substrate was then dissolved in a bath containing chromic and sulfuric acid. The composition determination and the magnetoresistance studies of the deposits were carried out after removing their substrates.

Elemental analysis of the multilayers was performed using energy dispersive X-ray (EDX) analysis. The composition of several regions of the deposits was determined and an average of these values was taken.

Magnetoresistance measurements were carried out at room temperature in the central part of the multilayer samples using four point contacts arranged in a square [2] in magnetic fields up to 8 kOe. The fields were applied approximately parallel and perpendicular to the direction of the current flowing in the film plane to measure the longitudinal and transverse magnetoresistance, respectively, as described in previous work [2, 5]. In each case, the percentage change in the resistance, MR(%), as a function of the applied magnetic field was calculated according to the relation $MR(\%) = \{[R(H) - R_{min}]/R_{min}\} \times 100$, where $R(H)$ is the value of the resistance at any magnetic field and R_{min} is the value at the field where the resistance is minimum.

3. Results and discussion

3.1. *Electrochemical characterisation*

In order to obtain preliminary information about the deposition processes and to choose the appropriate deposition potentials, the solution was first characterized by cyclic voltammetry (CV). The stabilized CV curves (second or further cycles) obtained for solutions of pH = 3.3 with and without Cu are shown in Figures 1(a) and (b), respectively. The potential sweep rate was 20 mV s^{-1} and the size of the Cu working electrode was the same as during the multilayer deposition. The potential scan was started in the cathodic direction (from $+0.5$ to -1.5 V vs SCE). During the first cycle (not shown), dissolution of the Cu substrate was observed first as an initial anodic current, then a peak appeared in the cathodic side at around -0.2 V, corresponding to the reduction of Cu^{2+} ions. These features are no longer observed in the second and further runs. In the potential range between -0.4 and -0.8 V, a current plateau with low current occurs, indicating diffusion-limited Cu deposition when copper sulfate is present (Figure 1(a)). If the electrolyte is void of copper, the current remains zero until the onset of nickel deposition (Figure 1(b)). The cathodic current begins to increase after about -0.8 V, and rises steeply due to the deposition of Ni, and possibly also due to H_2 generation. After the reversal of the scan direction, the current follows the same potential dependence back to about -0.8 V as in the cathodic-going scan. The anodic peak seen at about $+0.2$ V is due to Cu dissolution. This peak does not appear in the absence of copper sulfate after the second cycle (Figure 1(b)). Since no nickel dissolution peak is observed, it can be concluded that the nickel remains passive. These results are in good agreement with the findings of Bradley et al. [27] in that the Ni dissolution starts at a potential which is by 1.2 V more positive than the Cu/Cu^{2+} equilibrium potential in the same solution.

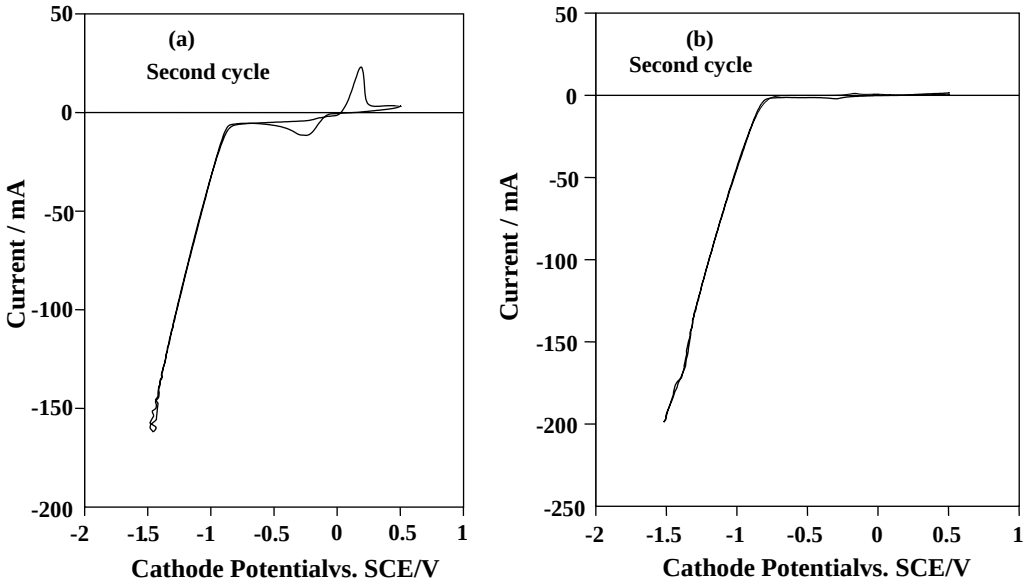

Fig. 1. (a) Cyclic voltammetry of the solution used to deposit Ni–Cu/Cu multilayers and (b) cyclic voltammetry of the solution having the same concentration as the multilayer solution but with no copper sulphate added. In both cases, the CV curves are shown for the second cycle after which the curves remained unchanged.

Based on the potentiodynamic measurements, the appropriate potential ranges to deposit Ni and Cu were estimated. The actual deposition potentials within these intervals were chosen to yield a deposit with a metallic appearance (shiny, mirror-like). Therefore, −0.2 and −1.7 V were selected for Cu and Ni deposition, respectively.

Figures 2(a) and (b) show the current-time transients recorded during growth for the first few layers of two multilayers with the same nominal layer thicknesses but grown at pH = 3.0 and 2.0, respectively. The composition of the samples and that of the magnetic layers are given in Table 1. The anodic current at the beginning of the deposition of the Cu layers arises from a capacitive transient. The Cu current changes with time from positive to a stable negative value until complete coverage of the underlying Ni layer with Cu. The instrumental transient was shorter than the data acquisition interval, and therefore all data points are meaningful.

As seen from Figure 2, the transient curves for Cu deposition have the same shape for the multilayers prepared at each pH value, while for Ni deposition they appear to have different shapes. The current for Ni deposition increases with time after an initial peak when

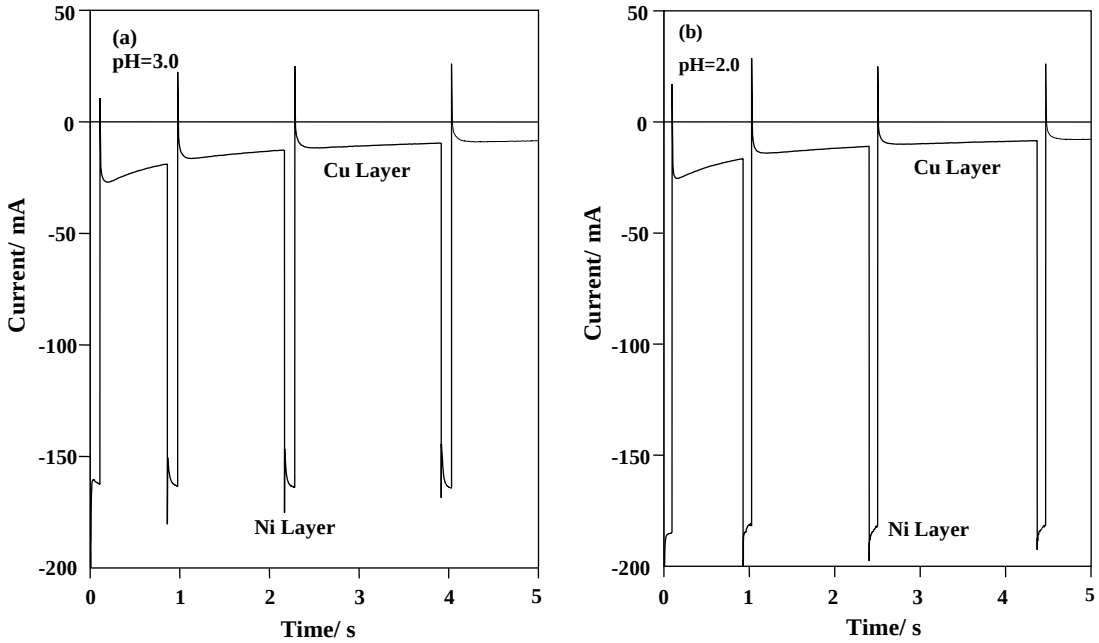

Fig. 2. Current transients for Ni–Cu/Cu multilayers grown from an electrolyte with (a) pH = 3.0 and (b) pH = 2.0.

Table 1. Elemental compositions of single Ni–Cu films and Ni-Cu/Cu multilayers grown at different electrolyte pH

	pH = 2.0		pH = 2.5		pH = 3.0	
	Cu (at.%)	Ni	Cu (at.%)	Ni	Cu (at.%)	Ni
Multilayer films 455[Ni–Cu(1.5 nm)/Cu(0.7 nm)]	39.0	61.0	45.3	54.8	52.0	48.0
Magnetic layers of the multilayers (calc.)	10.3	89.7	19.7	80.3	29.5	70.5
d.c. plated Ni–Cu films (1 μm)	7.7	92.3	17.8	82.2	28.6	71.4

the electrolyte pH is 3.0, while it decreases with time for pH 2.0. The current at the end of the Ni deposition pulse is the higher, the lower the pH. This indicates that the Ni layers have different growth modes for different pH. These results are similar to those observed in Ni–Co–Cu/Cu multilayers [15].

3.2. *Structural characterisation*

The structure of multilayers was studied by XRD measurements. Figure 3 shows the X-ray diffraction pattern of a multilayer with 500[Ni–Cu(2.0 nm)/Cu(2.0 nm)] grown on a (1 0 0) textured polycrystalline Cu substrate at high electrolyte pH (3.0). The peaks labeled Cu(2 0 0) and Cu(1 1 1) are the diffraction lines of the face-centered cubic (fcc) structure of the underlying substrate. Next to these peaks, the M(2 0 0) and M(1 1 1) peaks are the main Bragg peaks of the multilayer, corresponding to the average lattice spacing within the multilayer itself. For all samples studied, the (2 0 0) peaks of the multilayers are stronger than their (111) peaks. This indicates that the multilayers also have a strong (1 0 0) texture and an fcc structure like their substrates. The average interplanar distances of (2 0 0) and (1 1 1) planes were found to be (0.1795 ± 0.0088) and (0.2078 ± 0.0121) nm, respectively. These values are intermediate between the copper ones ($d_{2\,0\,0}$=0.1816 nm and $d_{1\,1\,1}$=0.2095 nm) calculated from Cu(2 0 0) and Cu(1 1 1) peaks of the XRD pattern (Figure 3) and the nickel ones ($d_{2\,0\,0}$=0.1762 nm and $d_{1\,1\,1}$=0.2035 nm) [28], indicating good coherency between the layers. The first order satellite peaks marked (+1) and (−1), which arise from the periodic structure of the multilayer, are clearly seen next to the multilayer M(2 0 0) peak. The modulation wavelength (the bilayer thickness of multilayer) was calculated to be (4.3 ± 0.2) nm from the satellite peak positions. This agrees fairly well with the nominal bilayer thickness (4.0 nm), which is the thickness calculated according to Faraday's law by assuming bulk densities and 100% current efficiencies for both Ni and Cu deposition. Similar results have been found for various repeat distances and for the entire pH range investigated. However, as the Ni layer thickness increases, the modulation wavelengths obtained from X-ray data were found to be slightly smaller than nominal bilayer

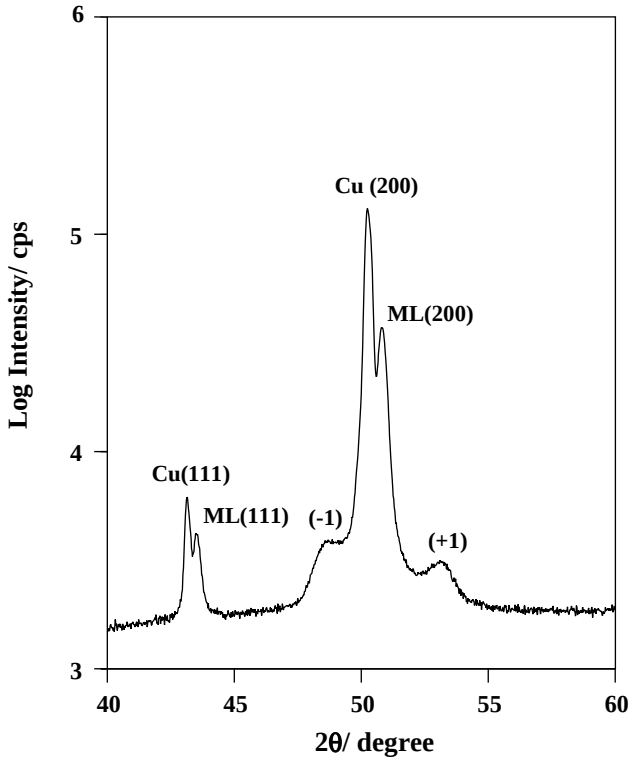

Fig. 3. XRD pattern of a multilayer with 500[Ni(2.0 nm)/Cu(2.0 nm)] grown on a (1 0 0) textured polycrystalline Cu substrate.

thicknesses. For example, the modulation wavelengths calculated from the XRD patterns for multilayers with 334[Ni–Cu(4.0 nm)/Cu(2.0 nm)] and 286[Ni–Cu(5.0 nm)/Cu(2.0 nm)] nominal thicknesses were found to be ~5.8 and ~6.6 nm, respectively. This trend is similar to that found for Ni–Cu/Cu multilayers deposited from a different electrolyte [22].

This difference in the nominal and measured bilayer repeats may be attributed to both hydrogen evolution occurring at the cathode during the reduction of Ni and the increase in surface roughness. As the Ni layer thickness, and hence the molar ratio of the Ni in the multilayer, increase the loss of the effective current during Ni deposition becomes more and more apparent. It is also reasonable that the larger the average current during the multilayer deposition, the more apparent is the surface roughening.

It should be noted that for any pH value satellite reflections were only observed for multilayers with Cu layer thicknesses at least as high as 2 nm, regardless of the Ni layer thickness. However, even below this Cu layer thickness the XRD patterns indicated the same crystal structure and texture as for the other multilayers. The lack of satellite reflections in these Ni–Cu/Cu multilayers differs from the result obtained previously on Ni–Co–Cu/Cu multilayers [15] where satellites were observed down to 0.8 nm Cu layer thicknesses at each pH value. The reason for this difference may lie in the different total multilayer thicknesses (0.3 μm in [15] and 2 μm here). It is well-known that the quality of multilayers degrades with increasing total thickness (e.g., the GMR was found to decrease [8] with increasing bilayer number for a constant bilayer repeat length). The reason is usually an evolution of the microstructure and the interface during growth. The necessity of a relatively large Cu layer thickness for the satellite peak observation is indirect evidence that roughening takes place during Ni deposition rather than during Cu deposition.

Figures 4(a) and (b) show the SEM micrographs of the multilayers with 455[Ni–Cu(1.5 nm)/Cu(0.7 nm)] nominal thickness grown at (a) pH=2.0 and (b) pH=3.0 on (1 0 0) textured polycrystalline Cu substrates. When the films were prepared at low pH (2.0), they had smoother surfaces compared to those prepared at high pH (3.0).

The chemical analysis results are summarized in Table 1. The first row shows the overall composition of Ni–Cu/Cu multilayers grown at three different pH values. The Cu layers can be assumed to consist of 100% Cu, thus the Cu content of the magnetic layers can be calculated using the nominal Ni–Cu and Cu layer thicknesses and these data are shown in the second row. The Cu content of the multilayer films and, therefore, that of the magnetic layers was found to increase with increasing pH. In order to check this composition change with varying pH, d.c. plated Ni–Cu films were grown for each pH at a constant potential of −1.7 V vs SCE, i.e., under the same electrochemical conditions as the magnetic layers in the multilayers. The d.c. plated Ni–Cu films had the same thickness as the nominal total thickness of the multilayers. As can be seen in the third row of Table 1, Cu content of the d.c. plated Ni–Cu films increased with electrolyte pH. This is the same trend as obtained for the magnetic layers from the overall analysed composition of the multilayers and even the quantitative agreement is fairly good. The increase in Cu content of multilayers, therefore, may be attributed to the increase in the Cu content of the magnetic layers. The increase in Cu content both in the d.c. plated films and in the multilayers with increasing electrolyte pH may be a result of the different growth mechanisms and/or chemical reactions at low and high pH.

This trend is anomalous in the sense that by lowering the hydrogen ion concentration in the electrolyte, an increase in the current efficiency of the nickel deposition is expected that would also lead to an increase in the Ni content of the deposit. The trend can rather be explained by a pH-dependent stability of the complex formed by nickel and sulphamate ions that also influences the transport properties of the electrolyte. From the data shown in Table 1, it can be concluded that the relative apparent transport rate of the metal ions depends on the pH, and the increase in hydrogen ion concentration facilitates the transport of nickel ions. Since anomalous nickel enrichment at low pH can also be observed in the d.c. deposits, the role of the exchange reaction in the enrichment can be excluded.

A similar increase in Cu content in the multilayer deposit with increasing pH was observed in electrodeposited Ni–Co–Cu/Cu multilayers [15]; this was mainly attributed to significant dissolution of Co and its replacement by Cu. Since the exchange reaction in our Ni–Cu/Cu multilayers is negligible, the same explanation should be applicable for the Ni–Co–Cu system as given here for the Ni–Cu system

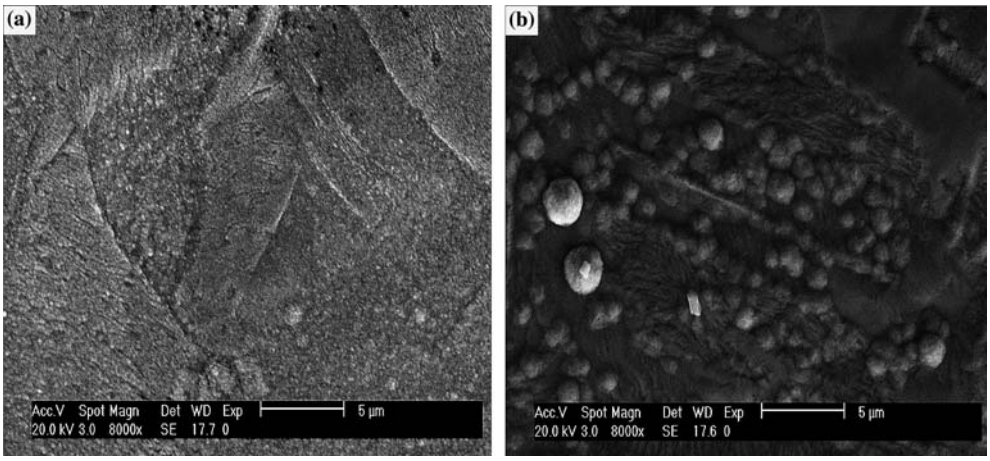

Fig. 4. SEM micrographs of the multilayers with 455[Ni–Cu(1.5 nm)/Cu(0.7 nm)] nominal thickness grown at (a) pH=2.0 and (b) pH=3.0 on (100) textured polycrystalline Cu substrates.

3.3. *Magnetoresistance characteristics*

Several samples were prepared for magnetoresistance measurements from electrolytes of different pH values such as 2.2, 2.6 and 2.9. The thickness of Ni layers was fixed at 1.5 nm, while the Cu layer thickness was changed between 0.4 and 2.0 nm. At each pH for multilayer films with Cu thicknesses less than 0.6 nm, the anisotropic magnetoresistance (AMR) effect of bulk ferromagnets [29] was found to be dominant. The AMR manifests itself as an increasing longitudinal and decreasing transverse magnetoresistance when the magnetic field increases from zero. This may be due to a percolation of the magnetic Ni–Cu layers with each other since the Cu layers at such very small thicknesses cannot completely separate them. The direct exchange coupling between the Ni-Cu layers leads to a ferromagnetic alignment of the magnetizations of neighbouring layers.

From 0.7 nm Cu layer thickness, the magnetoresistive response of the multilayers is already characteristic for GMR in that both the longitudinal and transverse magnetoresistance is negative in the whole range of magnetic field (Figure 5). It can also be seen that the magnetoresistance sharply decreases at low magnetic fields but does not saturate even in the maximum magnetic fields applied (±8 kOe).

In a recent paper [24], it has been demonstrated that the non-saturating behaviour of the magnetoresistance in electrodeposited Ni–Cu/Cu multilayers can be ascribed to the presence of superparamagnetic (SPM) regions whereas the central sharp peak arises from the ordinary ferromagnetic areas of the magnetic layers. Since in the present Ni–Cu/Cu multilayers the magnetoresistance curves show a rather continuous curvature in the whole range of magnetic fields, the observed magnetoresistance seems to be dominated by the contribution of SPM regions. This means that the multilayers with these Cu layer thicknesses can be rather considered as forming a granular type of metal: ferromagnetic Ni–Cu regions of size in the SPM regime [30] are dispersed in a non-magnetic Cu matrix. Since the thickness of these SPM regions can be taken as approximately equal to the average magnetic layer thickness, fairly large areas with lateral dimensions over 10 nm can already show SPM behaviour if they are decoupled from the rest of the magnetic layer or from other similar regions. The reason for decoupling can be interface intermixing, layer thickness fluctuation or uneven distribution of Cu and Ni in the magnetic layer. This implies that we have to deal with a multilayered structure in which the magnetic layers are not continuous over the whole sample volume (discontinuous multilayer). If the interface roughness is not too large, such partial discontinuities do not necessarily prevent the occurrence of XRD superlattice reflections.

The above described general behaviour was characteristic for multilayers deposited at each pH. The magnetoresistance curves (both transverse and longitudinal) of multilayers with the same nominal thicknesses 455[Ni–Cu(1.5 nm)/Cu(0.7 nm)] but grown at electrolyte pH values of 2.9 and 2.2 have already been shown in Figures 5(a) and (b) respectively. When comparing these two figures, it can be established that for both the longitudinal and transverse magentoresistance components the GMR values are smaller for pH=2.9 than for pH=2.2. The GMR values for identical multilayer samples prepared at pH=2.6 are intermediate between the data obtained for pH=2.2 and 2.9. Such an influence of the bath pH on the GMR magnitude is similar to that found for electrodeposited Ni–Co–Cu/Cu multilayers [15]. As discussed above, the electrolyte pH influences the surface and, hence, probably also the interface roughness and/or the crystallite size. These microstructural changes are all known to diminish the GMR.

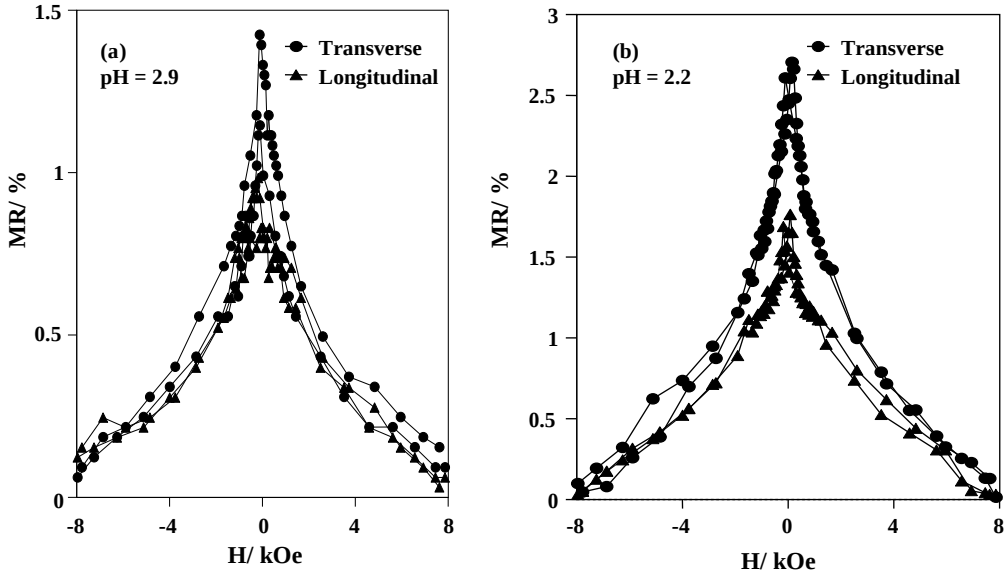

Fig. 5. Magnetoresistance curves for 455[Ni–Cu(1.5 nm)/Cu(0.7 nm)] multilayers grown from an electrolyte (a) pH=2.9 and (b) pH=2.2.

Another factor which may explain the influence of pH on the GMR magnitude in the present Ni–Cu/Cu multilayers is the change of Cu content with pH. The Cu content in the magnetic layers increases strongly with increasing pH, even up to nearly 30 at.% Cu for pH=3.0. On the other hand, it is well-known [31] that the Curie point (T_c) of Ni–Cu alloys decreases strongly with increasing Cu content (around 30 at.% Cu, T_c is already very close to 300 K). The lowered Curie temperature implies a reduction of the exchange splitting of the d-band electronic density of states (DOS). This reduction leads to a change in the Fermi level DOS values of the spin-down and spin-up subbands. Whereas in pure Ni the Fermi level intersects the spin-down DOS curve only (all the spin-up states lying at lower energies), the effect of strong alloying with Cu is that the Fermi level intersects both d-subband DOS curves. As a consequence, in terms of the two-current model, the spin asymmetry at the Fermi level which is responsible for spin-dependent transport processes in nanostructures is diminished and, hence, a smaller GMR results for higher Cu contents as observed.

4. Summary

We have electrodeposited Ni–Cu/Cu multilayers on (1 0 0) textured polycrystalline Cu substrates from an electrolyte with different pH values. It has been demonstrated that the multilayers have different growth modes for different electrolyte pH values and have the same crystal structure (fcc) and (1 0 0) texture as their substrates. It was found that the Cu content of magnetic layers increases with increasing electrolyte pH. The multilayers grown at high electrolyte pH (3.0) have rougher surfaces compared to those at low electrolyte pH (2.0). The GMR behaviour was found to be similar to that of granular type alloys in which the magnetic regions exhibit superparamagnetism. The estimated lateral size of the SPM regions would allow for a discontinuous multilayer structure. Furthermore, it was found that the films exhibit larger GMR values when they are grown from a low pH electrolyte. It has been shown that structural and compositional effects, both caused by the varying pH, can contribute to the observed changes in the GMR magnitude with pH.

Acknowledgements

This work was supported by the Scientific and Technical Research Council of Turkey (TÜBİTAK) under Grant no TBAG-1771. One of the authors (M.A.) thanks NATO for a Science Fellowship enabling a research stay at the Research Institute for Solid State Physics and Optics of the Hungarian Academy of Sciences where the MR measurements were performed. This part of the research was also supported by the National Scientific Research Fund (OTKA) of Hungary through grants F 032046 and T 037673. We also thank Prof. Hasan Mandal for the use of the X-ray diffractometer at TÜBİTAK-Ceramic Research Centre (University of Anadolu, Eskişehir).

References

1. C.A. Ross, *Ann. Rev. Mater. Sci.* **24** (1994) 159.
2. W. Schwarzacher and D.S. Lashmore, *IEEE Trans. Magn.* **32** (1996) 3133.
3. M. Alper, *Ph. D. Thesis*, University of Bristol, U.K. (1995).
4. T.P. Moffat, *Mater. Res. Soc. Symp. Proc.* **451** (1997) 413.
5. M. Alper, K. Attenborough, R. Hart, S.J. Lane, D.S. Lashmore, C. Younes and W. Schwarzacher, *Appl. Phys. Lett.* **63** (1993) 2144.
6. S.K.J. Lenczowski, C. Schönenberger, M.A.M. Gijs and W.J.M. de Jonge, *J. Magn. Magn. Mater.* **148** (1995) 455.
7. E. Tóth-Kádár, L. Péter, T. Becsei, J. Tóth, L. Pogány, T. Tarnóczi, P. Kamasa, I. Bakonyi, G. Láng, Á. Cziráki and W. Schwarzacher, *J. Electrochem. Soc.* **147** (2000) 3311.
8. L. Péter, Á. Cziráki, L. Pogány, Z. Kupay, I. Bakonyi, M. Uhlemann, M. Herrich, B. Arnold, T. Bauer and K. Wetzig, *J. Electrochem. Soc.* **148** (2001) C168.
9. S.S.P. Parkin, Z. G. Li and D. J. Smith, *Appl. Phys. Lett.* **58** (1991) 2710.
10. L. Péter, Z. Kupay, Á. Cziráki, J. Pádár, J. Tóth and I. Bakonyi, *J. Phys. Chem. B* **105**, (2001) 10867.
11. I. Bakonyi, J. Tóth, L. Goualou, T. Becsei, E. Tóth-Kádár, W. Schwarzacher and G. Nabiyouni, *J. Electrochem. Soc.* **149** (2002) C195.
12. W.R.A. Meuleman, S. Roy, L. Péter and I. Varga, *J. Electrochem. Soc.* **149** (2002) C479.
13. M. Shima, L. Salamanca-Riba, R.D. McMichael and T.P. Moffat, *J. Electrochem. Soc.* **149** (2002) C439.
14. G. Nabiyouni, O.I. Kasyutich, S. Roy and W. Schwarzacher, *J. Electrochem. Soc.* **149** (2002) C218.
15. M. Alper, W. Schwarzacher and S. J. Lane, *J. Electrochem. Soc.* **144** (1997) 2346.
16. G. Nabiyouni and W. Schwarzacher, *J. Magn. Magn. Mater.* **156** (1996) 355.
17. E. Chassaing, A. Morrone and J.E. Schmidt, *J. Electrochem. Soc.* **146** (1999) 1794.
18. V. Weihnacht, L. Péter, J. Tóth, J. Pádár, Zs. Kerner, C. M. Schneider and I. Bakonyi, *J. Electrochem. Soc.* **150** (2003) C507.
19. Á. Cziráki, J.G. Zheng, A. Michel, Zs. Czigány, G. Nabiyouni, W. Schwarzacher, E. Tóth-Kádár and I. Bakonyi, *Z. Metallkde.* **90** (1999) 278.
20. D.S. Lashmore, Y. Zhang, S. Hua, M.P. Dariel, L. Swartzendruber and L. Salamanca-Riba, *in* L.T. Romankiw and D.A. Herman, Jr. (Eds), 'Proc. 3rd Int. Symp. on Magnetic Materials, Processes, and Devices', Vol. 94-6 (Electrodeposition Division of The Electrochemical Society, Pennington, N.J., 1994 p. 205).
21. I. Bakonyi, E. Tóth-Kádár, T. Becsei, J. Tóth, T. Tarnóczi, Á. Cziráki, I. Gerõcs, G. Nabiyouni and W. Schwarzacher, *J. Magn. Magn. Mater.* **156** (1996) 347.
22. Á. Cziráki, I. Gerõcs, B. Fogarassy, B. Arnold, M. Reibold, K. Wetzig, E. Tóth-Kádár and I. Bakonyi, *Z. Metallkde.* **88** (1997) 781.
23. J. Tóth, L.F. Kiss, E. Tóth-Kádár, A. Dinia, V. Pierron-Bohnes and I. Bakonyi, *J. Magn. Magn. Mater.* **198–199** (1999) 243.
24. I. Bakonyi, J. Tóth, L.F. Kiss, E. Tóth-Kádár, L. Péter and A. Dinia, *J. Magn. Magn. Mater.* **269** (2004) 156.
25. W.R.A. Meuleman, S. Roy, L. Péter and I. Bakonyi, *J. Electrochem. Soc.* **151** (2004) C256.
26. D.S. Lashmore, R.R. Oberle, L.H. Bennett, L.J. Swartzendruber, U. Atzmony, M.P. Dariel and L.T. Romankiw, *in* L.T. Romankiw and D.A. Herman, Jr. (Eds), 'Proc. Int. Symp. on Magnetic Materials, Processes, and Devices' Vol. 90-8 (Electrodeposition Division of The Electrochemical Society, Pennington, N.J., 1990) p. 347.

27. P. Bradley, S. Roy and D. Landolt, *J. Chem. Soc., Faraday Trans.* **92** (1996) 4015.
28. B.D. Cullity, 'Elements of X-ray Diffraction', (Addison-Wesley Publishing Company, Inc, Reading. 1978), 2nd edition.
29. T.R. McGuire and R.I. Potter, *IEEE Trans. Magn.* **11** (1975) 1018.
30. B.D. Cullity, 'Introduction to Magnetic Materials', (Addison-Wesley, Reading. 1972).
31. I. Bakonyi, E. Tóth-Kádár, J. Tóth, T. Becsei, L. Pogány, T. Tarnóczi and P. Kamasa, *J. Phys.: Cond. Matter.* **11** (1999) 963.